

Adsorption of Tin Using Granular Activated Carbon

Kailas L. WASEWAR^{1*}, Shiv KUMAR² and B. PRASAD²

¹ Department of Chemical Engineering, Visveswarya National Institute of Technology (VNIT)
Nagpur - 440011, Maharashtra, India

² Department of Chemical Engineering, Indian Institute of Technology (IIT)
Roorkee – 247667, Uttarakhand, India

Abstract

Adsorption studies for removal of tin from the aqueous phase using granular activated carbon (GAC) and characterization of GAC were carried out. Particle size, proximate, ash, and ultimate analyses were carried out for the physiochemical characteristics of GAC. Thermogravimetric analysis was also done both in ambient and nitrogen atmospheres to see the effect of temperature on GAC stability. Morphological characteristics were given through scanning electron microscope analysis. The surface area of GAC was found to be 864.67 m²/g, and GAC worked as a very good adsorbent due to the presence of adsorption facilitating functional groups. The effects of various parameters like pH, adsorbent dose, initial concentration of tin, and temperature on adsorption performance was studied using GAC. The adsorption of tin by GAC followed pseudo-second order kinetics. Diffusion is not the only rate-controlling step. Adsorption equilibrium data were analyzed by the Langmuir, Freundlich, and Temkin isotherm equations. The Temkin isotherm was found to be best for tin adsorption onto GAC. Adsorption capacity of activated carbon for tin removal decreases with increase in temperature, the adsorbent showing the exothermic nature of adsorption. The high negative value of change in Gibbs free energy (ΔG°) indicates the feasible and spontaneous adsorption of tin onto GAC.

Keywords: Adsorption, tin, activated granular carbon, characterization, batch study, kinetics, equilibrium, thermodynamics.

JEPS (2009), Vol. 3, pp. 41 – 52.

1. Introduction

Over the past few decades, rapid industrialization has led to a tremendous increase in the use of heavy metals, which has inevitably resulted in an increased flux of metallic substances in the aquatic environment. Tin is one of the toxic metals found in most wastewaters. Many industries produce large quantities of waste streams containing low concentrations of tin, along with other metals from processes such as tin electroplating, aluminum anodizing, printed circuit board manufacturing, and metal pickling. Recycling metals from such solutions is attractive for environmental reasons and for the value of metals.

A level of tin (250 mg/kg) in canned food is generally accepted as a maximum tolerance level for humans. If a large amount of tin in canned food is taken daily over a long period, acute effects such as stomachaches, anemia,

and liver and kidney problems occur. The Occupational Safety and Health Administration (OSHA) has designated a workplace exposure limit of 0.1 mg/m³ for organic tin compounds, and 2 mg/m³ for inorganic tin compounds, except oxide. There are various treatment processes for removal and/or recovery of heavy metal ions, including precipitation, oxidation, ultrafiltration, electrodialysis, solvent extraction, ion exchange, adsorption etc. [1]. For high strength and low volumes of wastewater, heavy metal removal by adsorption is a good proposition. Granular activated carbon (GAC) is the most widely used adsorbent, as it has good capacity for the adsorption of carcinogenic metals.

In view of environmental aspects, it is essential to remove tin from wastewater to the desired concentration. This paper describes the investigation that has been carried out to study the removal of tin from the aqueous phase by adsorption using GAC. Characterizations of GAC, batch study, equilibrium, kinetic, and thermodynamic studies were carried out. Also the error analysis was reported to select the best isotherm.

*To whom all correspondence should be addressed: Tel: 91-712-2801561; Fax: 91-712-2223230; E-mail: k_wasewar@rediffmail.com; k_wasewar@che.vnit.ac.in

2. Model and Parameter Estimation

2.1. Kinetics Model

Various models are available to explain the kinetics of adsorption. To investigate the adsorption process of Sn (II) onto GAC, three kinetic models were used: pseudo- first-order, pseudo-second-order, and intraparticle diffusion.

The Lagergren rate equation is one of the most widely used sorption rate equations to present the adsorption process. The pseudo-first-order equation is [2]:

$$\frac{dq}{dt} = k_f (q_e - q) \quad (1)$$

where q is the amount of adsorbate adsorbed at time t (mg/g), q_e is the adsorption capacity in equilibrium (mg/g), k_f is the rate constant of the pseudo-first-order model (1/min), and t is the time. After definite integration by applying initial conditions at $t = 0, q = 0$, and $t = t, q = q$, the equation becomes:

$$\log(q_e - q) = \log q_e - \frac{k_f}{2.303} t \quad (2)$$

The straight line plot of $\log(q_e - q)$ against t for Sn (II) gives the value of adsorption rate constant (k_f) of Sn (II) with GAC.

The pseudo-second-order model can be represented in the following form [3]:

$$\frac{dq}{dt} = k_s (q_e - q)^2 \quad (3)$$

where k_s is rate constant of the pseudo-second-order model (g/mg min). After integrating equation boundary conditions at $t = 0, q = 0$, and $t = t, q = q$, the following form of the equation is obtained:

$$\frac{t}{q} = \frac{1}{k_s q_e^2} + \frac{1}{q_e} t \quad (4)$$

The initial sorption rate in mg/gm min, as $t \rightarrow 0$ can be defined as

$$\left(\frac{dq}{dt} \right)_{initial} = k_s q_e^2 \quad (5)$$

The initial sorption rate, the equilibrium adsorption capacity (q_e), and the pseudo-second-order rate constant k_s can be determined from plot of t/q versus t .

An empirically found functional relationship, common to most adsorption processes, is that uptake varies almost proportionally with $t^{1/2}$, the Weber Morris plot, rather than with the contact time t [4]:

$$q = k_{id} t^{1/2} + C \quad (6)$$

Where k_{id} is the intraparticle diffusion rate constant, values of intercept C give an idea of the thickness of the boundary layer.

2.2. Isotherm Models

Freundlich [5], Langmuir [6], Redlich-Peterson [7], and Temkin [8] isotherm models were used to describe the equilibrium characteristics of adsorption of tin onto GAC. Linearized form of Freundlich isotherm is given as:

$$\ln q_e = \ln K_F + \frac{1}{n} \ln C_e \quad (7)$$

Linearized form of Langmuir isotherm is given as:

$$\frac{C_e}{q_e} = \frac{1}{K_L q_m} + \frac{C_e}{q_m} \quad (8)$$

The Redlich-Peterson model combines elements of the Langmuir and Freundlich models. The mechanism of the Redlich-Peterson adsorption model is a hybrid and does not follow ideal monolayer adsorption. The Redlich-Peterson isotherm has a linear dependence on concentration in the numerator and an exponential function in the denominator. It approaches the Freundlich model at high concentrations and is in accordance with the low concentration limit of the Langmuir equation. Furthermore, the Redlich-Peterson model incorporates three parameters into an empirical isotherm, and therefore can be applied either in a homogeneous or heterogeneous system due to the high versatility of the equation. It can be described as follows:

$$q_e = \frac{K_R C_e}{1 + a_R C_e^\beta} \quad (9)$$

where K_R and a_R are Redlich-Peterson isotherm constants (lit/mg) and β is the exponent, which lies between 1 and 0, where $\beta = 1$

$$q_e = \frac{K_R C_e}{1 + a_R C_e} \quad (10)$$

It becomes a Langmuir equation, when $\beta = 0$

$$q_e = \frac{K_R C_e}{1 + a_R} \quad (11)$$

Equation (11) can be linearized as in equation (12).

$$\ln\left(K_R \frac{C_e}{q_e} - 1\right) = \ln a_R + \beta \ln C_e \quad (12)$$

The equation parameters were determined by minimizing the distance between the experimental data points and the theoretical model predictions with the solver add-in function of Microsoft Excel.

The Tempkin isotherm contains a factor that explicitly takes in account adsorbing species- adsorbate interactions. This isotherm assumes that (i) the heat of adsorption of all molecules in the layer decreases with coverage due to adsorbate-adsorbent interaction, and (ii) adsorption is characterized by a uniform distribution of binding energies, up to some maximum binding energy. The Tempkin isotherm is represented by the following equation:

$$q_e = \frac{RT}{b} \ln(K_T C_e) \quad (13)$$

Equation (13) can be linearized as in equation (14).

$$q_e = B_1 \ln K_T + B_1 \ln C_e \quad (14)$$

Where $B_1 = \frac{RT}{b}$

Regression of q_e versus $\ln C_e$ enables the determination of isotherm constants K_T and B_1 . K_T is an equilibrium binding constant (lit/mg) corresponding to the maximum binding energy, and constant B_1 is related to the heat of adsorption.

2.3. Error Analysis

Due to the inherent bias resulting from linearization, five different error functions of non-linear regression basin [sum of the square of the errors (SSE), sum of the absolute errors (SAE), average relative error (ARE), hybrid fractional error function (HYBRID), and Marquardt's percent standard deviation (MPSD)] were employed in this study to find out the best-fit isotherm model to the experimental equilibrium data [9,10].

SSE is given as:

$$SSE = \sum_{i=1}^n (q_{e,estm} - q_{e,exp})_i^2 \quad (15)$$

Here, $q_{e,estm}$ and $q_{e,exp}$ are, respectively, the estimated and the experimental value of the equilibrium adsorbate solid concentration in the solid phase (mg/g), and n is the number of the data point. This is the most commonly used error function. SSE has one major drawback in that it will result in the calculated isotherm parameters providing a better fit at the higher end of the liquid phase concentration range. This is because of the magnitude of the errors, which increases as the concentration increases.

SAE is given as:

$$SAE = \sum_{i=1}^n |q_{e,estm} - q_{e,exp}|_i \quad (16)$$

The isotherm parameters determined by this method provide a better fit as the magnitude of the errors increases, biasing the fit towards the high concentration data.

ARE is defined as

$$ARE = \frac{100}{n} \sum_{i=1}^n \left| \frac{(q_{e,exp} - q_{e,estm})}{q_{e,exp}} \right|_i \quad (17)$$

This error function attempts to minimize the fractional error distribution across the entire concentration range.

HYBRID is given as

$$HYBRID = \frac{100}{n-p} \sum_{i=1}^n \left[\frac{(q_{e,exp} - q_{e,estm})}{q_{e,exp}} \right]_i \quad (18)$$

This error function was developed to improve the fit of the ARE method at low concentration values. Instead of n as used in ARE, the sum of the fractional errors is divided by $(n-p)$ where p is the number of parameters in the isotherm equation.

MPSD has been used by a number of researchers in the field to test the adequacy and accuracy of the model fit with the experimental data. It has some similarity to the geometric mean error distribution, but was modified by incorporating the number of degrees of freedom. This error function is given as:

$$100 \sqrt{\frac{1}{n-p} \sum_{i=1}^n \left(\frac{(q_{e,exp} - q_{e,estm})}{q_{e,exp}} \right)_i^2} \quad (19)$$

2.4. Thermodynamic Study

Thermodynamic data, such as adsorption free energy, can be obtained from both Langmuir and Tempkin equations:

$$-\Delta G^{\circ} = RT \ln (K) \quad (20)$$

The thermodynamic parameters for adsorption of Sn (II) were calculated by using following equations:

$$\left. \begin{aligned} -\Delta G_{ads}^{\circ} &= RT \ln(K) \\ \Delta H^{\circ} &= -R \left[\frac{T_2 T_1}{(T_2 - T_1)} \right] \ln \frac{K_{L_2}}{K_{L_1}}, \\ \Delta S^{\circ} &= -\frac{(\Delta G^{\circ} - \Delta H^{\circ})}{T} \end{aligned} \right\} \quad (21)$$

Where K , K_{L_1} , and K_{L_2} are the equilibrium constants at temperatures T , T_1 , and T_2 , respectively, obtained from Langmuir or Tempkin isotherms.

3. Materials and Methods

3.1. Adsorbent and its Characteristics

GAC prepared from bagasse was used. The physicochemical characteristics of GAC were determined using standard procedures. A proximate analysis of the GAC was carried out using the procedure as per IS 1350:1984. The bulk density of GAC was determined using a MAC bulk density meter.

X-Ray diffraction analysis of GAC was carried out using the Phillips (Holland) diffraction unit (Model PW1140/90). The scanning electron microscope (SEM) analysis was carried out using the LEO 435 VP scanning electron microscope.

The ultimate CHN analysis was performed on finely ground and oven-dried GAC to determine the weight fractions of carbon, hydrogen, and nitrogen. The weight fractions of carbon, hydrogen, and nitrogen were determined using the Perkin Elmer CHN elemental analyzer.

Thermal degradation of (pyrolysis and gasification) of the GAC was studied using the thermo gravimetric and differential analysis techniques. The thermal decomposition of GAC was carried out non-isothermally in a pyres diamond TG/TGA of Perkin Elmer Instruments. The samples were prepared carefully to obtain homogeneous material properties. The degradation runs were taken at a heating rate of 20 °C/min under an inert atmosphere (flowing nitrogen) for pyrolysis and an oxidizing atmosphere (flowing moisture free air) for gasification. The test was conducted from ambient temperature to 1,000 °C. Flowing rate in both cases was kept constant at 200 ml/min. The thermo gravimetric (TG), differential thermo gravimetric (DTG), and differential thermal analysis (DTA) curves obtained in each case were analyzed to understand the behavior of thermal degradation.

3.2. Adsorbate and its Measurement

The adsorbate, tin chloride (SnCl_2), was supplied by RANBAXY Fine Chemicals Limited, India. It was used without any treatment. Experimental solutions of the desired metal concentrations were prepared by successive dilution with distilled water. The range of concentration 500-2,000 mg/lit was used. Concentration of Sn (II) was determined by Atomic Absorption Spectroscopy.

A GBC AVANTA atomic absorption spectrometer (AAS) operating with an air-acetylene flame and equipped with a cathode on Sn-hollow cathode lamp at 4 and 6 mA current settings, respectively, was employed. The pH measurements were performed by using a Senso Direct SN 651720 model pH meter combined with a glass electrode. Containers were shaken during the adsorption experiments by a water bath shaker (REMI Equipments Limited, India) set to 150 rpm at constant temperature.

3.3. Batch Study

To study the effect of different parameters, the batch operations were found to be most suitable. Batch adsorption experiments were carried out in a 100-ml stoppered conical flask for removal of tin from the aqueous phase using GAC. For optimum amount of adsorbent per unit mass, adsorbate in 50 ml aqueous solution was agitated separately with different GAC doses until equilibrium was reached. The solution pH (2-14), contact time (0-330 min), initial metal concentration (500-2,000 mg/l), GAC dose (1-8 g/l), and temperature (288-333 K) were varied. The solutions were filtered and the remaining concentrations of metal ions after adsorption were determined by atomic absorption spectrometer.

4. Results and Discussion

4.1. Characterization of GAC

The physicochemical characteristics (proximate analysis, ash analysis, particle size analysis, XRD analysis, ultimate analysis, etc.) of GAC are given in Tables 1 to 3. GAC has a high bulk density. GAC has a high surface area of 864.67 m^2/g , which comprises mainly the pore surface area, with an average pore diameter of 25.42 Å. Particle size is important in systems having external mass transfer resistance. The aqueous solution-adsorbent mixture was agitated at the maximum rpm, and external mass transfer resistance was assumed to be absent.

Adsorption of tin is basically governed by intra-particle surface diffusion, where pore size distribution and surface area are important. Average particle size of GAC is 3-5 μm . For structural and morphological characteristic, SEM analysis and XRD were carried out. Many crevices and holes within particles were found almost everywhere in the GAC. The d-value characteristics of GAC are presented in Table 3. From an XRD pattern, the major components identified in GAC were $\text{Fe}_2(\text{SO}_4)_9\text{H}_2\text{O}$ and $\text{Pb}_5\text{Cl}(\text{ASO}_3)_3$, and the major peak indicates the presence of silica in the

form of tridynite and alpha cristobalite compounds. Diffraction peaks corresponding to crystalline carbon were not observed in the GAC.

Table 1. Physical and chemical properties of GAC used	
<i>Characteristic</i>	<i>Values</i>
Proximate analysis (sample as received)	
Moisture (%)	7.23
Ash (%)	9.28
Volatile matter (%)	5.20
Fixed carbon (%)	78.29
Bulk density (kg/m³)	720.52
Ultimate analysis (dry basis)	
C	79.16
H	5.185
N	0.045
S	0.541
O	15.24
Chemical analysis of ash (%)	
Insoluble matter	3.2
Silica	2.9
Ferric & alumina	3.6
CaO	88.0
Mg	2.5
Surface area (m²/g)	
BET	864.67
Langmuir	1045.43
t-plot micropore	985.29
t-plot external	56.14
Single point	883.19
BJH adsorption cumulative	79.16
Pore volume (cm³/g)	
Single point pore volume	0.59
t-plot micropore volume	0.36
BJH adsorption cumulative	0.08
Pore size (Å)	
BET adsorption average pore width	25.42
BJH adsorption average pore diameter	45.00

Table 2. Particle Size Analysis of GAC	
<i>Sieve Size (BSS)</i>	<i>Weight %</i>
> 10	0.92
10-16	4.39
16-18	8.85
18-30	9.42
30-60	33.54
60-100	26.05
< 100	6.83

Table 3. XRD Analysis of GAC	
2θ	d (Å)
6.200	14.244
8.650	10.214
26.807	3.323
32.249	2.773
44.809	2.021
55.470	1.655
61.911	1.497
70.668	1.332
87.018	1.119
98.497	1.017

6.200	14.244
8.650	10.214
26.807	3.323
32.249	2.773
44.809	2.021
55.470	1.655
61.911	1.497
70.668	1.332
87.018	1.119
98.497	1.017

The FTIR spectra of GAC display a number of adsorption peaks, indicating the complex nature of the GAC. The FTIR spectroscopic analysis indicated broad bands at 3,414 cm⁻¹, representing bonded -OH groups. The bands observed at about 2,966-2,847 cm⁻¹ could be assigned to the C-H stretch. The peaks around 1,638-1,565 cm⁻¹ correspond to the C=O stretch. The C-O band absorption peak is observed to shift around 1,070 cm⁻¹. Thus, it seems that this type of functional group is likely to participate in metal binding.

The degradation characteristics of GAC were determined under a flowing air and nitrogen atmosphere, as obtained by TG, DSC, and DTG for a heating rate of 25 °C/min. The degradation runs were taken under an inert atmosphere (flowing nitrogen) for pyrolysis and an oxidizing atmosphere (flowing moisture free air) for gasification. Tests were conducted from ambient temperature to 1,000 °C. Flowing rate in both cases was kept constant at 200 mL/min. Under an air atmosphere, the moisture removal of 6.77% was observed to occur up to 100 °C followed by removal of light volatiles up to 250 °C. This initial zone was followed by the active pyrolysis (second degradation) zone from 250 to 500 °C with total degradation of 74.14 %. The subsequent degradation was found to proceed very slowly beyond 600 °C, with total degradation of 1.75%. Residue left at 985 °C was ash and constituted about 2% of the original sample.

Thermal degradation characteristics in a flowing nitrogen atmosphere showed removal of moisture and light volatile of about 10.2% up to a temperature of 200 °C. It was followed by two active degradation zones between 200-350 °C and 350-500 °C, degradation in the first zone was 33.95% and in the second zone was 22.12%. Subsequent degradation was very slow and went beyond 1,000 °C. This shows that granular activated carbon is very stable up to 250 °C and can be used as a fixed bed adsorbent.

4.2 Batch Study

4.2.1. Effect of Adsorbent Dose

The effect of GAC dose for removal of Sn (II) from 500 mg/l of metal solution at a temperature of 303K for contact

time of 330 min is shown in Figure 1. It can be observed that the percent of adsorption increases with GAC dose increase from 1 to 12 g/L solution. Increase in adsorption with adsorbent dose can be attributed to increased adsorbent surface area and availability of more adsorption sites. The optimum value of adsorbent dose was found to be 8 g/L of solution. The same was used for further studies.

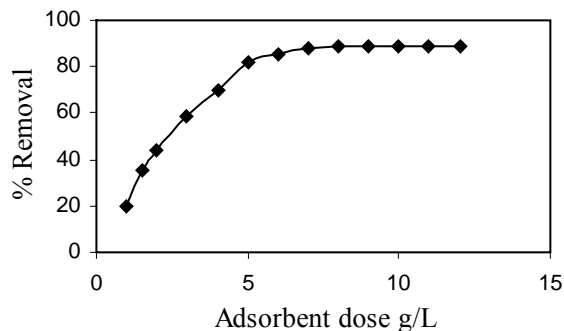


Figure 1. Effect of adsorbent dosage on the adsorption of tin using GAC (pH = 4, GAC dosage = 1-12 g/L, initial conc. = 500 mg/L, Temp. = 303 K, time = 330 min)

4.2.2. Effect of Solution pH

The pH of the aqueous solution is an important controlling parameter in the heavy metal adsorption process; thus, the role of hydrogen ion concentration was examined from solutions at different pH, covering the range of 2-14. The effect of solution pH on removal of Sn (II) from 500 mg/L metal solution, using GAC of 8 g/L of solution at a temperature of 303K for contact time 330 min, is shown in Figure 2. Tin ion exists in different forms in aqueous solution and the stability of these forms is dependent on the system's pH. The maximum removal of tin was observed at a pH of 4, and the same was considered for further study.

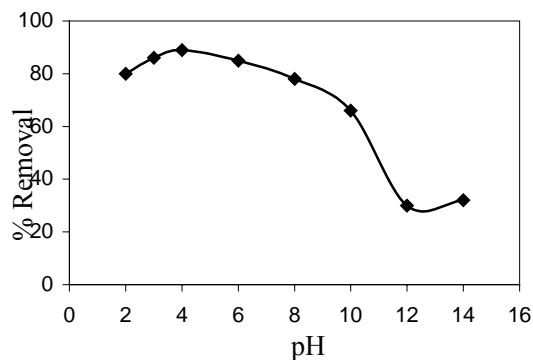


Figure 2. Effect of pH on the adsorption of tin using GAC (pH = 2-14, GAC dosage = 8 g/L, initial conc. = 500 mg/L, Temp. = 303 K, time = 330 min)

At lower pH values, the H^+ ions compete with metal cations for the exchange sites in the system, thereby partially realizing the latter, which compete with the Sn^{2+} ions for the adsorption sites of GAC. Decrease in

adsorption at higher pH was due to the formation of soluble hydroxyl complexes. The heavy metal cations were completely released under circumstances of extreme acidic conditions.¹¹

4.2.3. Effect of Contact Time

Contact time between the metal and the adsorbent is of significant importance in wastewater treatment by adsorption. Rapid uptake of metal and establishment of equilibrium in a short period signifies the efficiency of an adsorbent for its use in wastewater treatment.

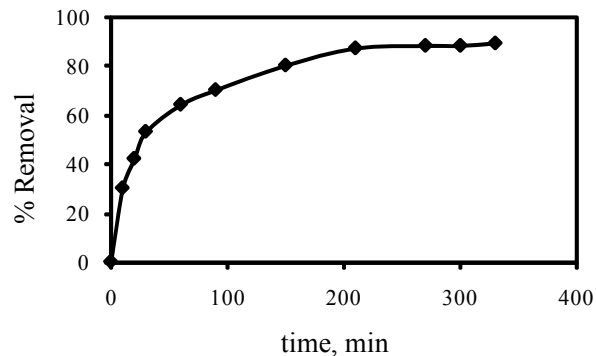


Figure 3. Effect of contact time on the adsorption of tin using GAC (pH = 4, GAC dosage = 8 g/L, initial conc. = 500 mg/L, Temp. = 303 K, time = 0 - 330 min)

Figure 3 shows the percentage removal of Sn (II) for 500 mg/L of initial concentration of tin by GAC (8 g/L) at different contact times.

The contact time curve shows that removal was very rapid in the first 75 minutes, then the adsorption rate gradually decreased and removal reached equilibrium at around 330 minutes. It was also observed that the time required to reach equilibrium depended on the initial concentration of tin. For the same concentration, the percentage removal of tin increased with increase in contact time until equilibrium was attained in 30 minutes. The curves are single smooth and continuous leading to saturation. These curves indicate the possible monolayer coverage of metal on the surface of the GAC.

4.2.4. Effect of Initial Concentration of Tin

A given mass of adsorbent can adsorb only fixed amount of adsorbate. So the initial concentration of adsorbate solution is important. Figure 4 shows the percentage removal of Sn (II) by GAC (8 g/L) at different contact times for various initial concentrations (500-2,000 mg/L) of tin. It can be seen that the percent adsorption decreased with increase in initial concentration, but the actual amount of Sn (II) adsorbed per unit mass of adsorbent (GAC) increased with increase in initial concentration in test solution. This was because of the decrease in resistance for the uptake of solute from solution with increase in metal concentration.

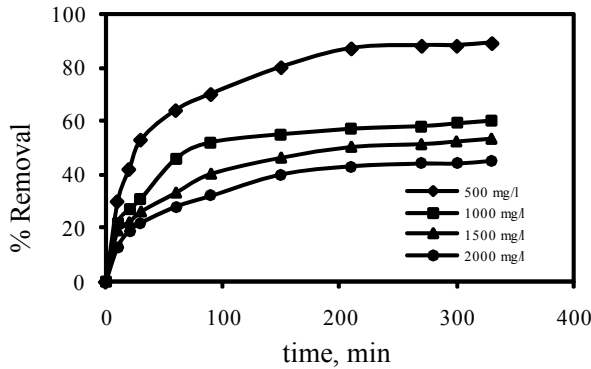


Figure 4. Effect of initial concentration of tin on adsorption of tin using GAC (pH = 4, GAC dosage = 8 g/L, initial conc. = 500 – 2,000 mg/L, Temp. = 303 K, time = 0 - 330 min)

4.2.5. Effect of Temperature

Adsorption studies were carried out at four different temperatures—288, 303, 318, and 333K. Since adsorption increased at higher temperatures, Sn (II) adsorption on GAC is exothermic in nature. The details of the effect of temperature can be obtained in the literature.¹² The increase of adsorption yield and adsorption capacity at increased temperature indicated that the adsorption of Sn (II) ions by GAC may involve not only physical but also chemical sorption. This effect may be due to the fact that at higher temperatures, an increase in active sites occurs due to bond rupture [13].

4.3. Kinetic

Various kinetic models (pseudo-first-order, pseudo-second-order, and intraparticle diffusion model) were used to find out the best fit kinetic model for the adsorption of Sn (II) on GAC. The plot of $\log(q_e - q)$ against t for the pseudo-first-order model (equation (3)) is shown in Figure 5 for different initial concentrations (500-2,000 mg/L). The straight line plot shows the validity of this model. The values of adsorption rate constant (k_f) of Sn (II) with GAC are given in Table 4. These values indicate that the adsorption rate was very fast at the beginning of adsorption of tin onto GAC.

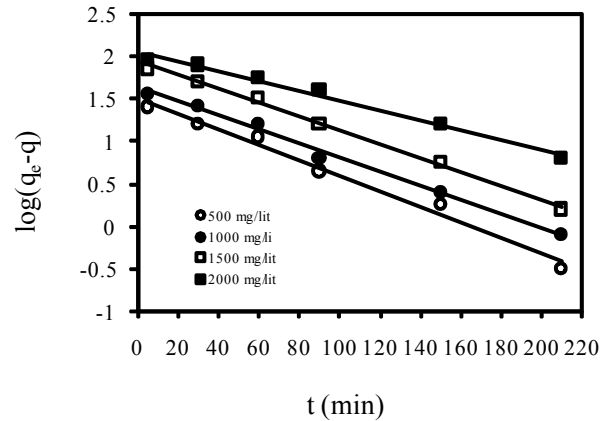


Figure 5. Pseudo-first-order kinetic plot for adsorption of tin onto GAC (pH=4, GAC dosage = 8 g/L, initial conc. = 500 to 2,000 mg/L, Temp. = 303 K)

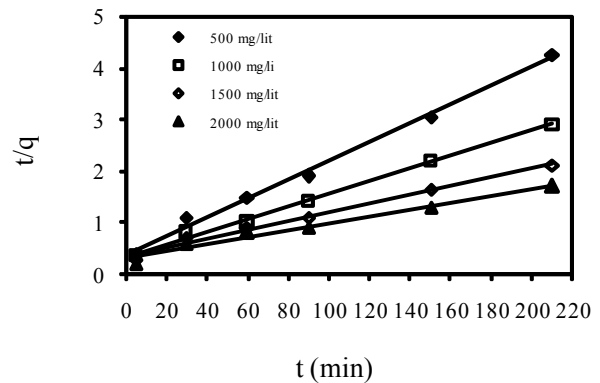


Figure 6. Pseudo-second-order kinetics plot for adsorption of tin onto GAC (pH=4, GAC dosage = 8 g/L, initial conc. = 500 to 2,000 mg/L, Temp. = 303 K)

Kinetic results were also presented in the form of the pseudo-second-order model (equation (5)) in Figure 6. Correlation coefficient for both pseudo-first-order and pseudo-second-order models were estimated using regression analysis. Kinetic constants are given in Table 3.

Table 4. Kinetic parameters for removal of tin by adsorption onto GAC

Conc. (mg/lit)	Pseudo-first-order			Pseudo-second-order				Intra-particle diffusion					
	k_f (1/min)	q_e (mg/g)	R^2	k_s (g/mg min)	q_e (mg/g)	h (mg / g min)	R^2	$k_{id,1}$ (mg/g min)	$k_{id,2}$ (mg/g min)	C_1	C_2	R_1^2	R_2^2
500	0.0230	31.83	0.9860	0.00084	55.25	2.567	0.9943	3.181	0.801	15.91	40.856	0.9845	0.9913
1,000	0.0191	42.48	0.9927	0.000461	81.30	3.047	0.9960	4.604	1.509	22.04	52.621	0.9899	0.9898
1,500	0.0187	86.56	0.9966	0.00021	117.65	2.878	0.9879	6.711	2.629	19.89	62.161	0.9973	0.9979
2,000	0.0134	114.47	0.9862	0.00015	149.25	3.288	0.9734	7.237	4.962	23.86	49.912	0.9895	0.9865

Table 5. Equilibrium isotherm parameters for adsorption of Sn (II) onto GAC

Temp. (°K)	Freundlich			Langmuir				Redlich-Peterson				Tempkin		
	K_F (mg/g)/(mg/L) ^{1/n}	1/n	R^2 (linear)	K_L (L/mg)	q_m (mg/g)	R_L	R^2	K_R (L/g)	a_R (L/mg)	β	R^2	K_T (L/mg)	B_1	R^2
500	17.7254	0.2566	0.9845	0.0224	87.7193	0.0820	0.9873	1.5	0.0153	1.0595	0.9883	0.5533	14.881	0.9810
1,000	20.8676	0.2662	0.9940	0.0296	103.0928	0.0633	0.9833	6.5	0.1439	0.9060	0.9937	0.8523	16.59	0.9652
1,500	31.3433	0.2803	0.9681	0.1064	162.2791	0.0185	0.9981	12.3	0.1164	1.0025	0.9970	2.2300	19.637	0.9842
2,000	41.1531	0.2939	0.9452	0.3717	119.0476	0.0054	0.9994	36.0	0.2522	1.0592	0.9976	6.7034	20.557	0.9692

Since correlation coefficients were found to be more close to unity for the pseudo-second-order model than for the first-order model, sorption reaction was better approximated by the pseudo-second-order kinetics model. The pseudo-first-order and pseudo-second-order kinetics models could not identify the diffusion mechanism, so the kinetic results were analyzed using the intraparticle diffusion model (Weber-Morris Model). According to this model, the plot of uptake versus the square root of time should be linear if intraparticle diffusion is involved in the adsorption process. If these lines pass through the origin, then intraparticle diffusion is the rate-controlling step [14]. When the plots do not pass through the origin, this indicates some degree of boundary layer control and further shows that intraparticle diffusion is not the only rate-limiting step—other kinetic models may also control the rate of adsorption, and they all may be operating simultaneously [15].

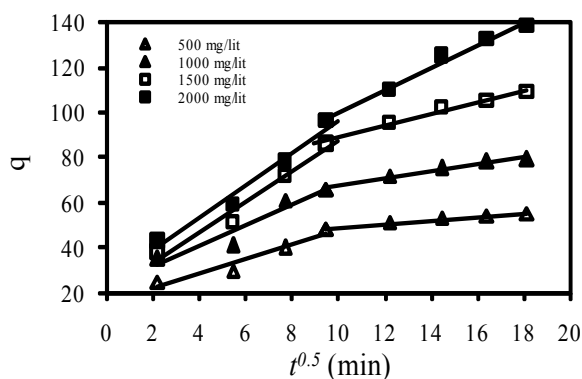


Figure 7. Weber Morris plot (intra-particle diffusion kinetic model) for adsorption of tin onto GAC (pH=4, GAC dosage = 8 g/L, initial conc. = 500 to 2,000 mg/L, Temp. = 303 K)

The adsorption kinetic data were fitted in the intraparticle diffusion model (equation (6)) as shown in Figure 7. Information on the thickness of the boundary layer can be obtained from the values of intercept C i.e., the larger the intercept, the greater the boundary layer

effect [16]. Deviation of the straight line from the origin may be due to a difference in the initial and final stages of adsorption. Further, such deviation indicated that pore diffusion was not the sole rate-controlling step [17]. Also, it was observed that there were two separate regions: the initial portion attributed to bulk diffusion, and the linear portion attributed to intraparticle diffusion. The values of $k_{id,1}$ and $k_{id,2}$ as obtained from the intercepts of the straight lines are listed in Table 4. Again, it may be suggested both film and pore diffusion were effective in the removal process to different extents. The macro pore diffusion rate was much larger than the micro pore diffusion rate.

The correlation coefficients for pseudo-first-order, pseudo-second-order, and intraparticle diffusion models were greater than 0.9860, 0.9734, and 0.9845, respectively. The correlation coefficients for the pseudo-first-order model were higher than those of the pseudo-second-order and intraparticle diffusion models.

4.4. Equilibrium Isotherms

The simplest adsorption isotherm is based on the assumptions that every adsorption site is equivalent and the ability of a particle to bind there is independent of whether adjacent sites are occupied [18]. Various equilibrium isotherm models were used for the equilibrium modeling of adsorption of Sn(II) onto GAC.

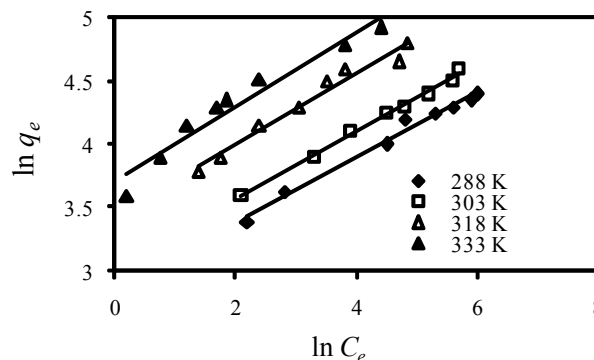


Figure 8. Freundlich adsorption isotherm for adsorption of tin onto GAC (pH=4, GAC dosage = 8 g/lit, Initial conc. = 500 to 2,000 mg/lit, Temp. = 288 – 333 K)

Table 6: Error analysis for equilibrium isotherms for adsorption of Sn (II) onto GAC						
Temperature	Isotherm	HYBRID	MPSD	SSE	SAE	ARE
288 K	Langmuir	6.5685	21.2463	124.8624	45.7571	12.2735
	Freundlich	0.3381	4.1002	32.1973	12.1626	2.5761
	R-P	16.633	3.5535	28.6911	47.8923	13.9215
	Tempkin	0.1117	5.6805	61.4188	17.5898	3.9047
303 K	Langmuir	4.9335	19.0652	136.5858	40.6176	9.4560
	Freundlich	0.5521	3.8624	43.9733	15.4193	2.9272
	R-P	26.2144	13.8277	38.9843	23.7211	6.8854
	Tempkin	0.1046	6.9928	86.6549	22.6629	4.9557
318 K	Langmuir	0.4336	5.6293	81.2371	20.8282	3.1926
	Freundlich	0.6152	11.2588	157.9343	47.8508	8.3830
	R-P	0.1262	7.2097	28.9157	26.9157	4.9055
	Tempkin	0.9115	7.3277	109.4052	24.3661	4.6916
333 K	Langmuir	1.4113	5.3828	60.8535	19.3852	3.5717
	Freundlich	73.7734	64.4423	169.1269	43.7542	55.3346
	R-P	5.1726	11.7212	46.8533	54.2377	7.9967
	Tempkin	0.2166	11.0453	186.6549	47.2377	8.1285

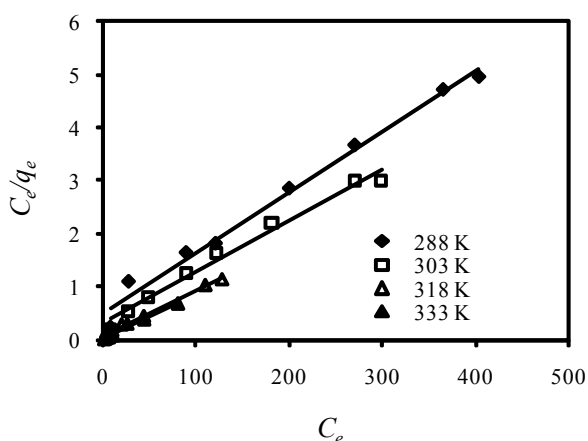


Figure 9. Langmuir adsorption isotherm for adsorption of tin onto GAC (pH=4, GAC dosage = 8 g/lit, Initial conc. = 500 to 2000 mg/lit, Temp. = 303 – 333 K)

According to the Langmuir model, the maximum Sn(II) adsorption capacity was obtained at 333 K, with a value of 119.05 mg/g. The results revealed that the

sorption capacity increased from 87.72 to 119.05 mg/gm with a temperature increase of 288 to 333 K. It was clear that the sorption of Sn(II) onto GAC was an endothermic process. The effect of temperature was fairly common and increased the mobility of the metal cation. Furthermore, increasing temperatures may produce a swelling effect within the internal structure of the GAC enabling the metal cation to penetrate further [20].

The Redlich-Peterson isotherm is shown in Figure 10. The Redlich-Peterson isotherm parameters and correlation coefficients were significantly higher than both Langmuir and Freundlich values for Sn (II) adsorption onto GAC. The values of the isotherm constant are presented in Table 5. The Redlich-Peterson was the best fit isotherm of the three isotherms studied. The Tempkin isotherm for Sn (II) is also plotted in Figure 11 and the isotherm constant values are presented in Table 5. As seen in Table 5, a decrease in the temperature produced a decrease in the adsorption capacity in all models. The values indicated that the adsorption pattern for Sn(II) onto GAC followed the Freundlich isotherm ($R^2 > 0.9452$), Langmuir isotherm ($R^2 > 0.9833$), Redlich-Peterson isotherm ($R^2 > 0.9883$), and Tempkin isotherm ($R^2 > 0.9652$) for all experimental

temperatures. On the basis of correlation coefficient R^2 , it was clear that the Langmuir and Redlich-Peterson isotherms best fit the sorption of Sn(II) onto GAC at various temperatures.

It is known that the magnitude of the Freundlich constant indicates a measure of the adsorbent capacity [21]. The values of n , as indicated in Table 5, were in the range of 3.4 to 3.9, indicating favorable adsorption. Results indicated that the capacity of GAC for sorption of Sn(II) incre

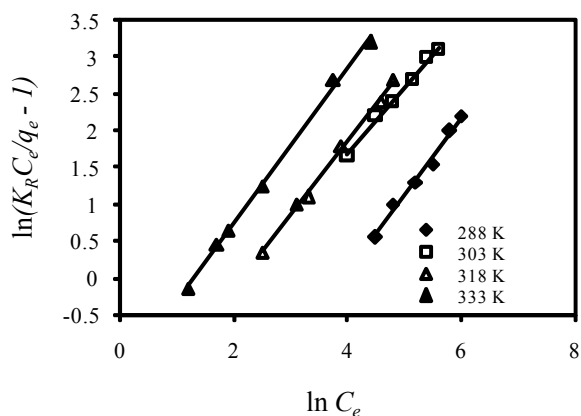


Figure 10. Redlich-Peterson adsorption isotherm for adsorption of tin onto GAC (pH=4.2, GAC dosage = 0.2 g/50 ml, initial conc. = 50 mg/lit, Temp. = 303 K)

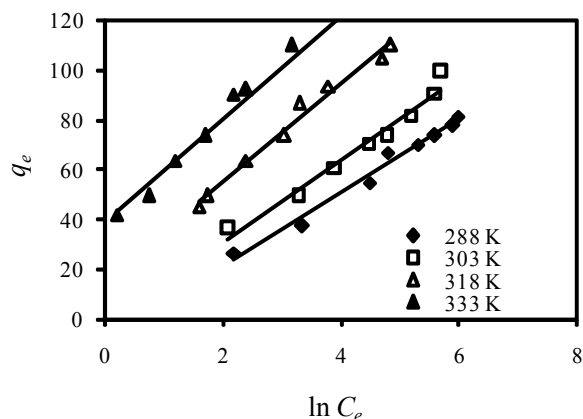


Figure 11. Temkin adsorption isotherm for adsorption of tin onto GAC (pH=4, GAC dosage = 8 g/lit, Initial conc. = 500 to 2,000 mg/lit, Temp. = 303 – 333 K)

ases with temperature, which was typical for the adsorption of most metal ions from their solution. When the system was in a state of equilibrium, the distribution of Sn(II) between the GAC and the Sn(II) solution was of fundamental importance in determining the maximum sorption capacity of GAC for the tin ion from the isotherm [22].

The effect of isotherm shape can be used to predict whether a sorption system is ‘favorable’ or unfavorable.’ The essential characteristics of a Langmuir isotherm can

be expressed in terms of a dimensionless factor, R_L , which describes the type of pattern and is defined as $R_L = 1/(1 + K_L C_i)$ (where C_i is the initial concentration and K_L is the Langmuir constant) and indicates the nature of adsorption as [23]:

If	$R_L > 1$	Unfavorable
	$R_L = 1$	Linear
	$0 < R_L < 1$	Favorable
	$R_L = 0$	Irreversible

The values of R_L less than 1, as given in Table 5, demonstrate that the adsorption can be deemed favorable. At all studied temperatures, the R_L values decreased with increasing initial tin ion concentration. This indicated that sorption was more favorable for the higher initial tin concentration than for the lower one.

4.5. Error Analysis of Equilibrium Isotherm

It is very difficult to select the best-fitting adsorption isotherm. Therefore, five different error functions [sum of squares of the errors (SSE), sum of the absolute errors (SAE), average relative error (ARE), hybrid functional error function (HYBRID), and Marquardt’s Percent Standard Deviation (MPSD)] of non-linear regression basin were employed to determine the best-fitting isotherm model to the experimental equilibrium data. The values of the five error functions are presented in Table 6. By comparing the error functions, it was found that the best-fitting isotherm follows the order: Langmuir > R-P > Freundlich > Temkin for Sn (II) adsorption onto GAC.

4.6. Thermodynamics

The thermodynamic parameters for adsorption of Sn (II) were calculated by using equations (20-21). The values of the thermodynamic parameters are given in Table 7. The enthalpy change ΔH° , and the entropy change, ΔS° for the sorption process were calculated to be 39.301 kJ/mol and 0.202 kJ/molK, respectively.

The negative value of free energy at each temperature indicated the feasibility of the process and the spontaneous nature of adsorption. The change in free energy decreased with increase in temperature, which indicated the endothermic nature of adsorption.

The endothermic nature of the adsorption process was well supported by the positive value of enthalpy change. The positive value of ΔS° reflects the affinity of the GAC for Sn(II) ions and suggests some structural changes in tin and GAC [23].

4.7. Disposal of GAC After Adsorption

In wastewater treatment systems using the adsorption process, the regeneration of the adsorbent and/or disposal of the loaded adsorbent are very important. It has been reported that the sorption process of trace metals is not reversible. Several explanations have been proposed in the literature [24].

GAC has a calorific value of about 14.5 MJ/kg. It can be utilized for making blended fuel briquettes, which could be used as furnace fuel. The bottom ash obtained after its combustion can be blended with cementitious mixtures. Setting and leaching tests on cementitious mixtures have shown that bottom ash can be incorporated into cementitious matrices to a great extent (75% of total solid) without risk of an unacceptable delay of cement setting and an excessive heavy metals leachability from solidified products [24,25]

Table 7. Thermodynamic parameters for adsorption of Sn(II) onto GAC

T(K)	ΔG° (kJ/mol K)	ΔH° (kJ/mol)	ΔS° (kJ/mol K)
288	-58.020	39.301	0.202
303	-61.044		
318	-64.068		
333	-67.092		

5. Conclusion

Adsorption studies for the removal of tin from the aqueous phase using GAC, and characterization of GAC, were carried out. Particle size, proximate, ash, and ultimate analyses were carried out for the physiochemical characteristics of GAC. Thermogravimetric analysis was also done both in ambient and nitrogen atmospheres to see the effect of temperature on GAC stability. Morphological characteristics are given through scanning electron microscope analysis. The surface area of GAC was found to be 864.67 m²/g, and GAC works as a very good adsorbent due to the presence of adsorption facilitating functional groups. BJH adsorption cumulative pore volume was 0.08 cm³/g, and t-plot micro pore volume was 0.36 cm³/g. BJH adsorption average pore diameter was 45 Å. Calorific value was 14.5 MJ/kg. From an XRD pattern, the major components identified in GAC were Fe₂(SO₄)9H₂O and Pb₅Cl(ASO₃), and a major peak indicated the presence of silica in the form of tridynite and alpha cristobalite compounds. Diffraction peaks corresponding to crystalline

carbon were not observed in GAC. FTIR studies revealed the presence of –OH, C-H, C=O, and C-O groups that participate in metal binding.

The effects of various parameters like pH, adsorbent dose, initial concentration of zinc, and temperature on adsorption performance were studied using GAC. The study showed the adsorption potential of GAC for the removal of Zn (II) from aqueous solution. The capacity of adsorption on Sn(II) increased with increasing temperature and pH. Adsorption capacity of GAC for Sn(II) removal increased with increase in temperature that may have happened due to the rapture of bond providing new adsorption sites. The maximum removal of tin was observed at a pH of 4. The maximum adsorption capacity of GAC was found to be 89% for adsorption of Sn(II).

Kinetic test results suggested that Sn(II) adsorption onto GAC followed pseudo-first-order-kinetics. The values indicated that the adsorption pattern for Sn(II) onto GAC followed the Freundlich isotherm ($R^2 > 0.9452$), Langmuir isotherm ($R^2 > 0.9833$), Redlich-Peterson isotherm ($R^2 > 0.9883$), and Tempkin isotherm ($R^2 > 0.9652$) at all experimental temperatures. On the basis of correlation coefficient R^2 , it was clear that the Langmuir and Redlich-Peterson isotherms were best-fitted for the sorption of Sn(II) onto GAC at various temperatures. Five different error functions [sum of squares of the errors (SSE), sum of the absolute errors (SAE), average relative error (ARE), hybrid functional error function (HYBRID), and Marquardt's Percent Standard Deviation (MPSD)] of the non-linear regression basin were employed to determine the best-fitting isotherm model to the experimental equilibrium data. It was found that the best-fitting isotherm follows the order: Langmuir > R-P > Freundlich > Tempkin for Sn (II) adsorption onto GAC.

The enthalpy change, ΔH° , and the entropy change, ΔS° , for the sorption processes were calculated to be 39.301 kJ/mol and 0.202 kJ/mol K, respectively. Positive ΔH° revealed the endothermic nature of adsorption, and the negative value of ΔG° showed the feasibility of adsorption. To recover its energy value, the metal-loaded GAC can be used to make fire-briquettes to be used in the furnaces. The resultant bottom ash can be blended with cementitious mixtures and then used as building blocks.

5. References

- [1] Aksu Z and Tunc O. (2005) Application of biosorption for penicilin G removal: comparison with activated carbon. *Process Biochemistry*; 40: 831-47.
- [2] Adriano WS, Veredas V, Santana CC and Goncalves LRB. (2005) Adsorption of amoxicillin on chitosan beads: kinetics, equilibrium and validation of finite bath models. *Biochemical Engineering Journal*; 27: 132-37.

- [3] Dutta M, Baruah R and Dutta NN. (1997) Adsorption of 6-aminopenicillanic acid on activated carbon. *Separation and Purification Technology*; 12: 99-108.
- [4] Dutta M, Baruah R, Dutta NN and Ghosh AC. (1997) The adsorption of certain semi-synthetic cephalosporins on activated carbon. *Colloid and Surfaces A*; 127: 25-37.
- [5] Kumar KV. (2007) Pseudo-second order models for the adsorption of safranin onto activated carbon : Comparison of linear and non-linear regression methods. *Journal of Hazardous Material*; 142: 564-67.
- [6] Silva FRC, Pereira JAM, Araujo MOD and Santana CC. (1999) Mass Transfer parameters evaluation in protein adsorption on macroporous resin. *Hungarian J. Ind. Chem*; 27: 183-87.
- [7] Bayrak Y, Yesiloglu Y, and Gecgel U. (2006) Adsorption behavior of Cr(VI) on activated hazelnut shell ash and activated bentonite. *Microporous and Mesoporous Materials*; 91: 107-10.
- [8] Tahir SS and Rauf N. (2006) Removal of a cationic dye from aqueous solutions by adsorption onto bentonite clay. *Chemosphere*; 63: 1842-48.
- [9] Banat FA, Al-Bashir B, Al-Asheh and Hayajneh O. (2000) Adsorption of phenol by bentonite. *Environmental Pollution*; 107: 391-98.
- [10] Chandra TC, Mirna MM, Surdayanto Y and Ismadji S. (2006) Adsorption of basic dye onto activated carbon prepared from durian shell: Studies of adsorption equilibrium and kinetics. *Chemical Engineering Journal*; 127: 121-29.
- [11] Hu QH, Qiao SZ, Haghseresht F, Wilson MA. and Lu GQ. (2006) Adsorption study for removal basic red dye using bentonite. *Ind. Eng. Chem; Res*: 733-38.
- [12] Koyuncu H. (2008) Adsorption kinetics of 3-hydroxybenzaldehyde on native and activated bentonite. *Applied Clay Science*; 38: 279-87.
- [13] Hameed BH, Din ATM and Ahmad AL. (2007) Adsorption of methylene blue onto bamboo-based activated carbon: Kinetics and equilibrium studies. *Journal of Hazardous Materials*; 141: 819-25.
- [14] Chen H and Wang A. (2007) Kinetic and isothermal studies of lead ion adsorption onto palygorskite clay. *Journal of Colloid and Interface Science*; 307: 309-16.
- [15] Ozcan AS and Ozcan A. (2004) Adsorption of acid dyes from aqueous solutions onto acid-activated bentonite. *Journal of Colloid and Interface Science*; 276: 39-46.
- [16] Hameed BH, Ahmad AA and Aziz N. (2007) Isotherms, kinetics and thermodynamics of acid dye adsorption on activated palm ash. *Chemical Engineering Journal*; 133: 195-203.
- [17] Ismadji S and Bhatia SK. (2000) Adsorption of flavour esters on granular activated carbon. *Canadian Journal Chemical Engineering*; 78: 892.
- [18] Ho YS and McKAY G. (1998) A comparison of chemisorption kinetics models applied to pollutant removal on various sorbents. *Trans IChemE*; 76B: 332-40.
- [19] Citraningrum M, Gunawan, Indraswati N and Ismadji S. (2007) Improved adsorption capacity of commercially available activated carbon norit ROW 0.8 Supra with thermal treatment for phenol removal. *Journal of Environmental Protection Science*; 1: 62-74.